

MICROMECHANISM CONTROLLING THE FATIGUE CRACK PROPAGATION IN Al-Zn-Mg SINGLE CRYSTALS

E. Affeldt and V. Gerold

Max-Planck-Institut für Metallforschung, Institut für Werkstoffwissenschaften, and Institut für Metallkunde der Universität Stuttgart D-7000 Stuttgart 1, Federal Republic of Germany

ABSTRACT

Stage I fatigue crack propagation has been studied in detail on an age-hardened Al-Zn-Mg single crystal. Plastic slip at the crack tip has been measured for dry environment conditions and found to be larger than the amount of crack propagation per cycle. The crack opening was very small. In wet environment the crack propagation rate is increased whereas plastic slip at the crack tip is negligible. A distinct crack opening exists even after compressing the specimen, which demonstrates a larger amount of secondary slip. The observed embrittlement may be caused by hydrogen diffusing into the persistent slip band in front of the crack tip. It also leads to an increased tendency for stage II crack propagation. A marked change in the fracture surface appearance with increasing crack propagation rate may be connected with the reduction of embrittlement at higher crack propagation rates.

KEYWORDS

Fatigue crack propagation; precipitation hardened alloy; stage I; plastic deformation; fracture surface; inert atmosphere; hydrogen embrittlement.

INTRODUCTION

Since the well-known paper by Forsyth (1962) it is accepted that in fcc metals and alloys two types of transcrystalline fatigue cracks are possible which are called stage I and stage II cracks. These two types differ in their crystallographic orientation which is caused by a different plastic behaviour near the crack tip. In most cases the fatigue crack develops from intrusions created by so-called persistent slip bands (PSBs) at the surface of the sample. The crack then follows such a band and can be observed running parallel to an active slip plane (stage I). Depending on the material and the circumstances the crack can later leave the active slip plane and develop a crack surface running mostly normal to the applied stress axis (stage II). In this case at least two different slip systems (without PSBs) inclined to the crack are active at its tip and cause crack propagation. The orientation of the crack

surface is no longer strictly crystallographic in that case.

Whereas much research has been reported on the behaviour of stage II cracks and many models have been proposed (Laird, 1967; Neumann, 1967) to describe the mechanism of stage II crack propagation the information on stage I crack propagation is much more limited, because stage I cracks occur less frequently and depend on several conditions. A stage I crack always needs a leading PSB in front of the crack tip. A PSB is only active as long as it is a soft area surrounded by a harder matrix. In single phase materials this difference is caused by a different dislocation structure as it has been observed in unnotched copper single crystals (Mughrabi, 1979; Winter, 1974) and polycrystals (Lukas and Klesnil, 1973). The difference in hardness remains small in that case. Such a PSB remains active as long as there is only a very small contribution of secondary slip. Due to the inhomogeneous stress distribution at a crack tip this is only the case for very low stresses resulting in a low crack propagation rate da/dN . For copper single crystals the maximum rate is about 1 nm/cycle for stage I crack propagation (Neumann, Fuhlrott and Vehoff, 1979).

For precipitation hardened alloys the situation can be quite different as long as shearable precipitated particles control the plastic deformation. In that case the localization of strain in PSBs leads to shear of the particles which finally ends in their dissolution within the band (Köhler, Steiner and Gerold, 1983; Vogel, Wilhelm and Gerold, 1982). This phenomena leads to a remarkable softening of the PSBs and can be observed macroscopically in a plastic strain controlled fatigue test. In single crystal experiments this softening effect is more evident. For Cu-Co it could be shown for example that the total amount of observed softening is about 80% of the precipitation hardening (Gerold and Steiner, 1982). In such cases the deformation via PSBs is stabilized even in complex stress fields at the crack tip where secondary slip systems are also active. As a result, stage I crack propagation can be observed up to 500 nm/cycle as has been found in this investigation.

In order to get more information on the nature of stage I crack propagation, an age-hardened Al-Zn-Mg alloy has been selected for this study. In addition, only single crystals were used. Such experiments have been reported already in the literature for the same alloy (Nageswararao and Gerold, 1967, 1977; Vogel, Wilhelm and Gerold, 1982) and for other alloys such as Ni base superalloys (Duquette and Gell, 1971, 1972; Gell and Leverant, 1968) or Cu-Co (Wilhelm, Nageswararao and Meyer, 1979). The main purpose of the present paper is to provide a more detailed investigation of the local deformation near the crack tip in order to find a model for stage I crack propagation. Since the moisture of the environment has a drastic effect on the cracking behaviour in Al alloys (Nageswararao and co-workers, 1977; Vogelesang and Schijve, 1980; Wei and co-workers, 1980) the study of its influence has also been included.

EXPERIMENTAL DETAILS

Single crystals of a high-purity alloy Al-5 wt% Zn - 1 wt% Mg were prepared by a strain-annealing technique. The rod-shaped crystals were machined by spark erosion into samples having a gauge length of 22 mm and a $8 \times 1.5 \text{ mm}^2$ cross section. The specimen axis was oriented for single slip with its broad surface being parallel to the Burgers vector of the primary slip system. The crystals were single edge notched with a notch depth of 0.5 mm. All crystals were homogenized at 480°C, quenched into water, and aged 4 days at 135°C. The stress-controlled fatigue experiments ($R = -1$) were performed in dry

nitrogen as well as in a nitrogen atmosphere with a relative humidity of 90%. The load was generated electro-dynamically and had a frequency of 50 Hz. The crack propagation was followed with a travelling microscope at a magnification of 200x; its position was recorded by a computer. To account for different orientations of the single crystals the crack propagation rate da/dN was always plotted as function of ΔK_{eff} with $\Delta K_{\text{eff}}^2 = \Delta K_{\text{I}}^2 + \Delta K_{\text{II}}^2$. Both quantities ΔK_{I} and ΔK_{II} have been calculated for the particular crack geometry according to Knott (1973) without, however, applying a correction function for the limited specimen size.

The plastic deformation in the crack-tip region was evaluated by SEM techniques in the following way: The crack propagation experiment with a measured propagation rate da/dN was stopped after the tension half cycle was finished and the load was zero. After taking several SEM pictures from the crack tip region the sample was again installed into the fatigue machine and the experiment was continued with the same rate for another 1000 cycles. Then the experiment was again stopped but this time when the compression half cycle was finished. Another set of SEM pictures was taken from the same areas. In both cases the PSB in front of the crack tip was slightly visible. The shear, S , at different places across the crack could be observed very easily from scratches crossing the crack at large angles. This displacement, S , was constant in the region of the crack tip and the PSB. The accuracy in S was better than 50 nm.

RESULTS

Dry Nitrogen Atmosphere

Experiments in a dry nitrogen atmosphere clearly show that the fatigue crack is propagating primarily in a stage I mode up to rates of $da/dN = 500 \text{ nm/cycle}$. The transition to a stage II mode always occurs at one or both of the broad surfaces of the crystal.

The stage I crack always follows a PSB which can be detected by SEM in front of the crack tip. The whole plastic deformation of the crystal is localized mainly in that band. Fig. 1 shows the SEM picture after unloading from the tension half cycle, which clearly shows the strain localization in the band (total slip $S_t = 300 \text{ nm}$). The crack seems to be totally closed thus making it difficult to detect the crack tip and the beginning of the PSB. A similar SEM picture after unloading the same crystal from the compression half cycle reveals no detectable slip in the PSB ($S_c = 0$). The resulting cyclic slip $\Delta S = S_t - S_c = 300 \text{ nm}$ is found to be about three times the crack propagation rate which is $da/dN = 100 \text{ nm/cycle}$ in this particular case (Fig. 2). It can be concluded that there exists a high reversibility of the localized shear in front of the crack. At higher rate values the ratio of ΔS to da/dN becomes smaller (Fig. 2).

The fracture surface of these slowly growing stage I cracks is quite flat and highly reflective as has been reported elsewhere (Duquette and Gell, 1971, 1972; Nageswararao and Gerold, 1967, 1977). With increasing propagation rates ($da/dN \approx 10 \text{ nm/cycle}$, Fig. 3) the surface becomes more and more structured and finally at a rate of 200 nm/cycle contains equiaxed dimples (Nageswararao and Gerold, 1967) (Fig. 4). They have a constant diameter of about 10 μm which does not vary with the propagation rate. However, the bordering walls of the dimples obviously increase in height with increasing da/dN . A thorough inspection discloses that the dimples have a flat surface

in their center surrounded either by walls or by valleys or by combination "walls plus valley". However, valleys and walls do not match on opposite fracture surfaces.

In addition, fracture steps are observed from the very beginning. At low propagation rates these steps are straight and relatively low. They run parallel to the active slip direction (Figs. 3,4). With increasing velocities the fracture steps converge and become noncrystallographic river lines aligned close to the direction of crack propagation. When they reach the specimen's surface the step results in the occurrence of two cracks propagating parallel to each other for a short distance (Fig. 5).

Wet Nitrogen Atmosphere

The crack propagation behaviour in wet nitrogen atmosphere is quite different from that in dry atmosphere. The most obvious effect is the simultaneous occurrence of stage I and stage II type cracks which can be observed in half of the experiments. For the case of pure stage I cracks there are also marked differences as follows: In a side view of the crack, a distinct opening displacement can be observed even after the compression half cycle is finished as it is shown in Fig. 6a. In contrast to this, Fig. 6b shows a side view of a crack which has propagated in dry nitrogen. In this case even after the tensile half cycle no opening can be detected at this magnification.

The crack surface also shows marked differences especially for low and medium crack propagation rates. Fig. 7 depicts an area where the crack propagating from right to left increases its rate from about 20 to 500 nm/cycle. On the right (low propagation rates) there is a flat surface which has nearly no structure. The area in the center part of the specimen is shown in Fig. 8 at a higher magnification showing a distinct roughness. Compared to Fig. 3 (dry atmosphere) the surface looks more brittle. In addition, this structure changes at areas near the edge of the specimen as shown in Fig. 9. More rough regions can be observed indicating noncoplanar deformation in planes normal to the fracture surface. Such differences never occurred for tests in the dry environment. The appearance of these brittle looking areas does not seem to be affected by the propagation rate. For higher rates a transition to a different behaviour is observed. It is characterized by a sharp narrow boundary structure (Fig. 7) which is always observed in wet atmosphere. Thereafter, the influence of the moisture diminishes. This change is correlated with irregularities in the log-log plot of da/dN versus ΔK occurring around 40 to 100 nm/cycle (Fig. 10). Finally, at propagation rates above 300 nm/cycle, a dimple-like structure is observed (Fig. 7) which is similar to that in the dry environment.

Stage II crack propagation is observed more often in wet nitrogen. This can be best observed if the environment is changed during the experiment. In Fig. 11 the crack propagates first in a dry atmosphere from the lower right to the upper left. Then the experiment was stopped and the atmosphere was changed to wet nitrogen. After continuing the cycling, the crack obviously leaves the slip plane and bends to a direction normal to the stress axis. After returning to dry atmosphere this stage II crack stops moving and the stage I crack starts to propagate again in its original plane. A later inspection of the fracture surface indicates that the deviation to stage II occurred along the whole crack front. After changing back to dry nitrogen a stage I crack forms in front of the first one and covers the whole fracture area again.

DISCUSSION

The occurrence of stage I fatigue cracks is connected with the existence of active PSBs developing during fatigue. Such bands are soft areas in a hardened matrix. The softer these areas are compared to the matrix the higher is the preference for stage I crack propagation. Obviously, this condition is fulfilled for age-hardened alloys as long as the precipitates are cut by dislocations during plastic deformation as has been mentioned already in the introduction. Even in the complex stress field at the tip of a crack one slip system will dominate and will form one or more PSBs in front of the crack tip which is then followed by the propagating crack. In a dry atmosphere this is the dominating mechanism in aluminium alloys, in particular in the Al-Zn-Mg system. The heavy shearing in the PSBs reduces the stress concentration at the crack tip and leads to a relatively low propagation rate because of a large amount of shear reversibility in the band as has been discussed already by Hornbogen and Zum Gahr (1976). The observed shearing amplitude ΔS is always larger than the propagation rate (Fig. 2). All attempts to model this crack propagation only by planar slip processes in these PSBs are futile. For example, the propagation model given by Laird (1978) is only an enlarging intrusion coupled with an enlarging equivalent extrusion. Obviously, a small amount of secondary slip is necessary in order to open the crack tip. Such secondary dislocations which have piled up at the borders of a PSB have been observed by TEM (Vogel, Wilhelm and Gerold, 1982). In Fig. 12 such a crack propagation model is sketched together with a plot of the corresponding stress-strain cycle. Fig. 12a depicts the situation in the first half of the tensile half cycle shortly before secondary slip sets in (at $\tau = \tau_{sec}$). The primary slip (for $\tau > \tau_{psb}$) has propagated the crack tip by ΔS . Thereafter, a small amount of secondary slip occurs which remains until the tensile half cycle has been finished (Fig. 12b). In the compression half cycle the crack propagation has partially reversed and a smaller final propagation Δa per cycle remains due to the secondary slip. Because of the anisotropic stress field around the crack tip the secondary shear will operate always at the same side of the crack. According to the model this may result in a small deviation of the crack from the slip plane (Δa is much larger than the secondary shear). The PSB in front of the crack tip either has to follow it or a new band is nucleated at the deviating crack tip.

In the wet environment the experimental results can be explained with the assumption that the wet atmosphere hardens the PSBs. The shearing in these bands is reduced and the stress concentration at the crack tip drastically increased. This leads to an increased activation of secondary slip which eventually becomes equivalent to primary slip and thus results in the onset of stage II crack propagation. A possible reason for the hardening in the PSBs can be that hydrogen produced at the crack tip diffuses into these bands and stops the continuous recovery processes necessary to keep the bands permanently soft. After returning to the dry environment the hardened PSB becomes active again and the crack starts to follow it as a stage I crack (see Fig. 11).

Since hydrogen production and diffusion is a thermally activated process the corresponding embrittlement is time dependent. Therefore, with increasing crack propagation rate its effect should be reduced. Since a reduction of this embrittlement reduces the speed of the propagating crack, embrittlement by hydrogen is increased and the crack speeds up and so on. When this critical situation is reached, a marked change of the crack appearance results as has been shown in Fig. 7. The sharp narrow line with high surface roughness marks the position of the crack tip where this effect occurs. At much larger propagation rates the embrittlement effect totally disappears. The final

dimple structure at the fracture surface is the same as in the dry environment.

REFERENCES

- Duquette, D.J., and M. Gell (1971). *Metall. Trans.*, **2**, 1325.
 Duquette, D.J., and M. Gell (1972). *Metall. Trans.*, **3**, 1899.
 Forsyth, P.J.E. (1962). In *Proc. Symp. on Crack Propagation*, Vol. 1, College of Aeronautics, Cranfield, Beds., p. 76.
 Gell, M., and G.R. Leverant (1968). *Acta Met.*, **16**, 553.
 Gerold, V., and D. Steiner (1982). *Scripta Met.*, **16**, 405.
 Hornbogen, E., and K.-H. Zum Gahr (1976). *Acta Met.*, **24**, 581.
 Köhler, E., D. Steiner and V. Gerold (1983). Effect of Cyclic Deformation on the Precipitation and Dislocation Structure of Al-1.8at.%Ag Single Crystals. In *Proc. 4th Risø Int. Symp. on Metallurgy and Materials*, p. 345.
 Knott, J.F. (1973). In *Fundamentals of Fracture Mechanics*, Butterworths, London.
 Laird, C. (1967). In *Fatigue Crack Propagation*, ASTM STP 415, p. 131.
 Laird, C. (1978). In *Fatigue and Microstructure*, Metals Park, Ohio, p. 149.
 Lukas, P., and M. Klesnil (1973). *Mater. Sci. Eng.*, **11**, 345.
 Mughrabi, H. (1979). In *Proc. ICSMA 5*, Vol. 3, Aachen, Pergamon, p. 1615.
 Nageswararao, M., and V. Gerold (1967). *Metall. Trans.*, **7A**, 1847.
 Nageswararao, M., and V. Gerold (1977). *Metal Science*, **11**, 31.
 Nageswararao, M., R. Meyer, M. Wilhelm, and V. Gerold (1977). In *Mechanisms of Environment Sensitive Cracking of Materials*, Surrey, 383.
 Neumann, P. (1967). *Z. Metallkde.*, **58**, 780.
 Neumann, P., H. Fuhlrott, and H. Vehoff. In *Fatigue Mechanisms*, ASTM STP 675, p. 371.
 Vogel, W., M. Wilhelm, and V. Gerold (1982). *Acta Met.*, **30**, 21.
 Vogel, W., M. Wilhelm, and V. Gerold (1982). *Acta Met.*, **30**, 31.
 Vogelesang, L.B., and J. Schijve (1980). *Fat. Eng. Mat. Struct.*, **3**, 85.
 Wei, R.P., P.S. Pao, R.G. Hart, T.W. Weir, and G.W. Simmons (1980). *Metall. Trans.*, **11A**, 151.
 Wilhelm, M., M. Nageswararao, and R. Meyer (1979). In *Fatigue Mechanisms*, ASTM STP 675, p. 214.
 Winter, A.T. (1974). *Phil. Mag.*, **30**, 719.

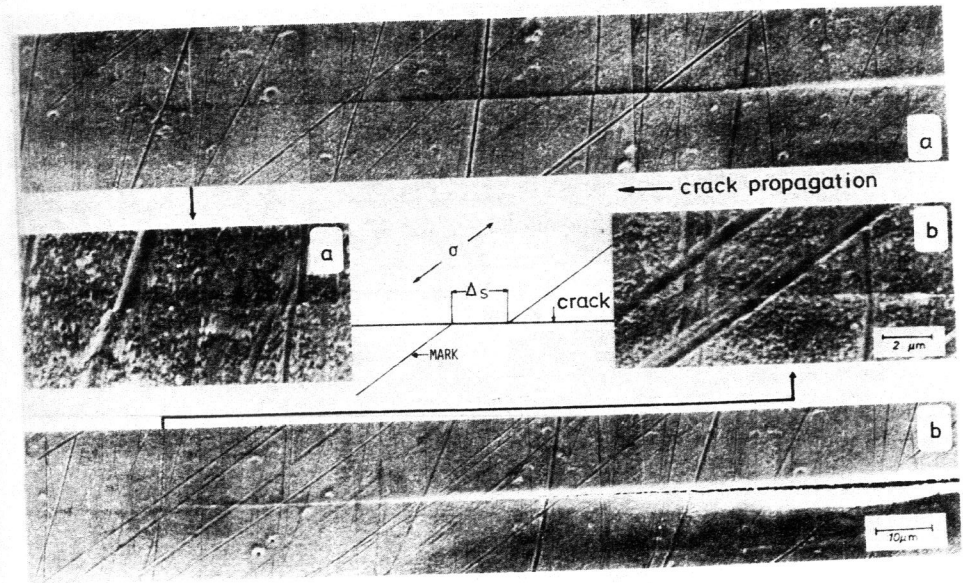


Fig. 1. Shear displacements S near the crack tip as measured by shifts in scratcher marks.

- a) after the tensile half cycle, $S_t = 300$ nm
 b) after the compression half cycle, $S_c = 0$ nm

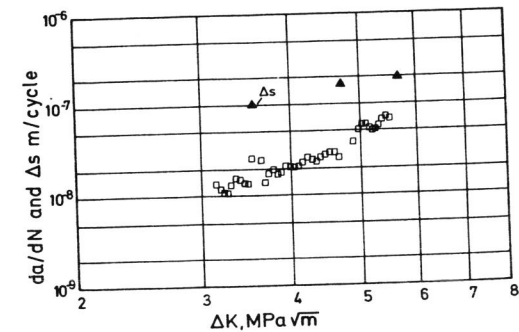


Fig. 2. Crack propagation rate and shear amplitude ΔS as a function of ΔK .

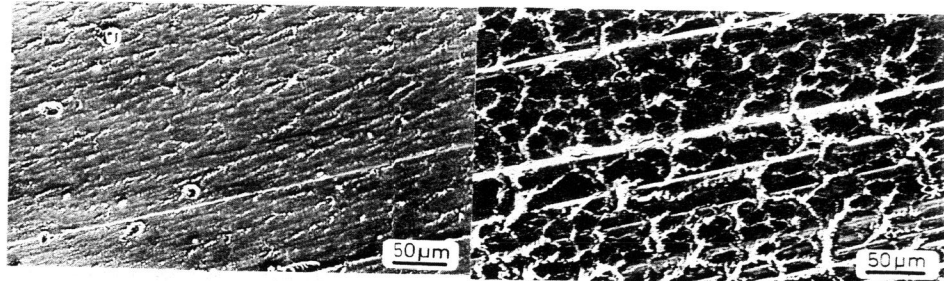


Fig. 3. Crack surface of a stage I crack in a dry nitrogen atmosphere at slow propagation rates ($da/dN = 10 \text{ nm/cycle}$).

Fig. 4. Crack surface of a stage I crack in a dry nitrogen atmosphere with crystallographic fracture steps ($da/dN = 200 \text{ nm/cycle}$).

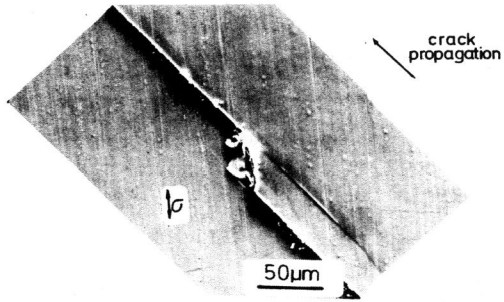


Fig. 5. Occurrence of two parallel cracks, as a river line reaches the specimen's surface.

Fig. 6. Crack opening

- a) in wet atmosphere stopped after a compression load.
- b) in dry atmosphere stopped after a tensile load.

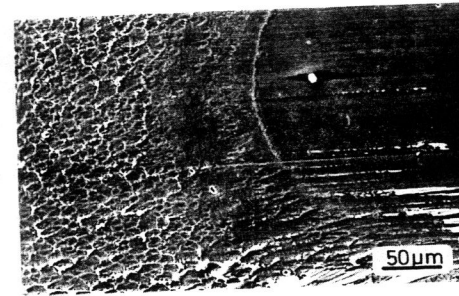
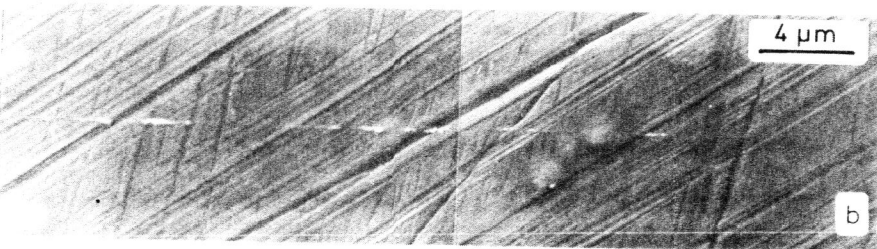
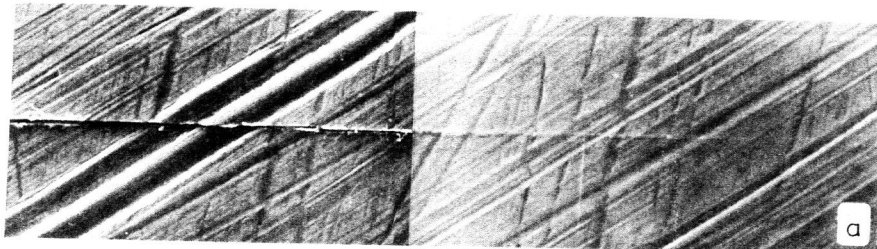


Fig. 7. Surface of a stage I crack in a wet atmosphere. The brittle part at the right side (low rate) ends in the described boundary structure. Thereafter, one can observe the well-known dimple-like structure as in a dry atmosphere.

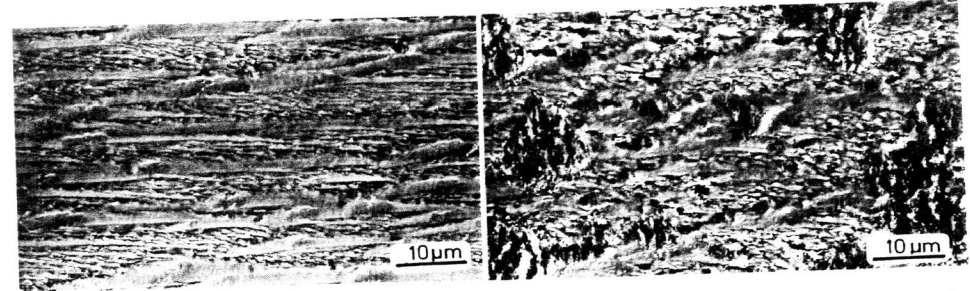


Fig. 8. Brittle part of a stage I fracture surface in a wet atmosphere. From the middle of the specimen ($da/dN = 10 \text{ nm/cycle}$).

Fig. 9. As Fig. 8. Near the edge of the specimen.

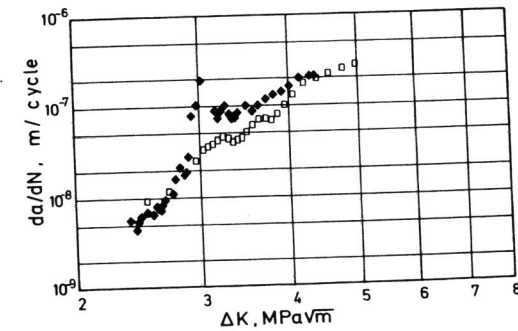


Fig. 10. Crack propagation rate of stage I cracks in a wet atmosphere. The discontinuity is correlated to the boundary structure, as shown in Fig. 7.

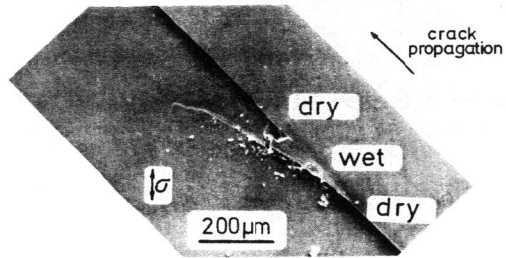


Fig. 11. A stage I crack propagating in a dry nitrogen atmosphere deviates from the slip plane as the atmosphere was changed to a relative humidity of 90%. As propagation was continued in dry nitrogen again, a new stage I crack starts from the PSB in front of the first one.

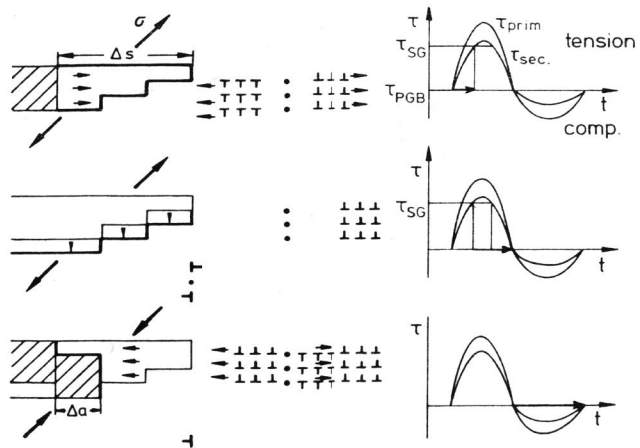


Fig. 12. The mechanism of stage I crack propagation. The hatched area marks the crack tip at the end of a full cycle.